JOURNAL OF GEOPHYSICAL RESEARCH, VOL. 116, D19119, doi:10.1029/2011JD015949, 2011

On the effective aerodynamic and scalar roughness length of Weddell Sea ice

Alexandra I. Weiss,[1] John King,[1] Tom Lachlan-Cope,[1] and Russ Ladkin[1]

Received 14 March 2011; revised 20 July 2011; accepted 24 July 2011; published 14 October 2011.

[1] We study the effective aerodynamic roughness length z_0_eff and scalar roughness length for temperature z_T_eff over different compact sea ice types in the Antarctic Weddell Sea by aircraft measurements during two austral summer seasons. z_0_eff and z_T_eff are highly variable in the Weddell Sea ice area. The averaged value of $\overline{z_T\text{\_eff}}$ in all main sea ice areas was smaller than the averaged value of $\overline{z_0\text{\_eff}}$. The ratio between the two roughness lengths was relatively small for new/young sea ice with $\overline{z_0\text{\_eff}}/\overline{z_T\text{\_eff}} \approx 2$, but the ratio became significantly large for the multiyear pack ice with $\overline{z_0\text{\_eff}}/\overline{z_T\text{\_eff}} \approx 227$. For the pack ice area, with sea ice concentration ranging between 95% to 100%, we determined a median $\overline{z_0\text{\_eff}} = 4.1 \times 10^{-03}$ m and a median $\overline{z_T\text{\_eff}} = 1.8 \times 10^{-05}$ m. In the new, young sea ice area, with sea ice concentration ranging between 98% and 100%, we observed a median $\overline{z_0\text{\_eff}} = \times 10^{-04}$ m and a median $\overline{z_T\text{\_eff}} = 2.2 \times 10^{-04}$ m. These values of $\overline{z_0\text{\_eff}}$ and $\overline{z_T\text{\_eff}}$ differ from published observations conducted in a pack ice and new, young sea ice area in the northern hemisphere, such as the Arctic. Most model parameterizations require the roughness lengths as constant values as boundary input parameters. Our study shows that by using the $\overline{z_0\text{\_eff}}$ and $\overline{z_T\text{\_eff}}$ values of this study, instead of commonly used sea ice roughness length values, the accuracy of parameterized heat and momentum fluxes in the Weddell Sea ice area can significantly be improved.

Citation: Weiss, A. I., J. King, T. Lachlan-Cope, and R. Ladkin (2011), On the effective aerodynamic and scalar roughness length of Weddell Sea ice, *J. Geophys. Res.*, *116*, D19119, doi:10.1029/2011JD015949.

1. Introduction

[2] Air-sea-ice interaction processes play an important role in the energy and water cycles of the polar regions. In the sea ice zone, sea ice influences the near-surface values of temperature, humidity and wind, whereby the fundamental links between air, sea and ice are radiation and the turbulent fluxes of sensible heat H, latent heat E and momentum τ. Most direct measurements of turbulent fluxes and the roughness lengths over sea ice have been conducted in the northern hemisphere [e.g., *Joffre*, 1983; *Overland*, 1985; *Garbrecht et al.*, 2002; *Schröder et al.*, 2003], while few such measurements are available for the Antarctic [e.g., *Wamser and Martinson*, 1993; *Andreas et al.*, 2005]. However, as Arctic and Antarctic sea ice have different physical characteristics, Antarctic measurements are essential for developing parameterizations that are appropriate for computing fluxes over Antarctic sea ice.

[3] Surface turbulent fluxes of heat and momentum are usually determined in climate and numerical weather prediction models by using a bulk parameterization. These parameterizations relate surface fluxes directly to readily available model variables, such as mean wind speed and temperature at the surface and at the lowest atmospheric model grid point. A prerequisite for the bulk parameterization approach is that the aerodynamic roughness length z_0 and scalar roughness length z_T, respectively, of the surface cover are known, because they are needed as integral constants. However, over heterogeneous surfaces the roughness lengths are not constant. They vary spatially and a whole spectrum of local roughness lengths normally exists. The sea ice zone in the western Weddell Sea is characterized by such a heterogeneous surface with a mixture of water and various sea ice types, ranging from smooth, young sea ice to very rough multiyear pack ice. Sea ice concentrations range from ice-free to totally ice-covered. *Rao et al.* [1974] described the influence of a sudden change in surface roughness on the boundary layer structure. Such distinct changes in the surface roughness and temperature lead for example to the development of internal boundary layers, as described, e.g., by *Garratt* [1990]. Close to the surface the turbulent flow is in equilibrium with the local surface and is thus horizontally variable. Above a certain height, known as the blending height [e.g., *Mason*, 1988; *Claussen*, 1991], the different internal boundary layers merge and the flow becomes independent of horizontal position. Above the blending height the turbulent heat fluxes can be assumed to be horizontally uniform [*Taylor*, 1987]. For a heterogeneous surface, which induces internal boundary layer development, effective values of the roughness lengths z_0_eff and z_T_eff can describe the surface roughness representative for a larger area, i.e., for an area the size of a

[1]British Antarctic Survey, National Environment Research Council, Cambridge, UK.

0148-0227/11/2011JD015949

Table 1. Measurement Capability of British Antarctic Survey Twin Otter Aircraft Equipped With Boundary Layer Instrumentation

Measurement Capability	Instruments
Total temperature	Goodrich Rosemount sensor 102 de-iced and normal
Dew point	Buck research 1011C cooled mirror
Airspeed	Static and pitot pressure, Honeywell HPA
Atmospheric turbulent fluxes	NOAA/ARA BAT probe running at 50 Hz
Position, altitude, attitude, velocity	JAVAD AT4: 4 GPS System at 20 Hz
Short wave radiation	Upward and downward looking Pyranometer, Eppley PSP
Long wave radiation	Upward and downward looking Pyrgeomenter, Eppley PIR
Infrared surface temperature	Downward looking Heimann, KT19.82
Video footage	Sony DV downward looking camcorder and cockpit handheld video

model grid box. The effective values can be calculated by using the parameter aggregation method. Over heterogeneous surfaces the magnitude of the effective roughness lengths differ in general from the local roughness lengths, as shown, e.g., by *Beljaars and Holtslag* [1991]. They showed that the area-averaged fluxes can be estimated in atmospheric models more accurately if the effective surface roughness length is known and a local value is not used. Contemporary regional weather and climate prediction models have a typical grid resolution of the order of 10 km in the horizontal dimension and the tendency is toward even finer grid cells. However, up to now there are only scanty experimental data on the effective roughness length of sea ice in the Antarctic, which could be used for numerical model studies of the ice-covered Southern Ocean. To fill in this knowledge gap, we conducted aircraft measurement in the area of the western Weddell Sea to determine effective roughness lengths over the heterogeneous sea ice zone. Aircraft measurements enable the direct determination of effective parameters for an area the size of a model grid box. In section 2 the aircraft instrumentation and the ice characteristics in the study area are presented. A summary of data processing and flight strategy as well as the measurement uncertainty is given in section 3. In section 4 we discuss our observations of the effective roughness lengths over sea ice. A discussion and summary of the main results of this study are given in section 5.

2. Experiment

2.1. Instrumentation

[4] For this study a DHC6 Twin Otter research aircraft operated by the British Antarctic Survey was equipped with instrumentation to measure boundary layer parameters. The core aircraft instrumentation used in this experiment is listed in Table 1. The maximum range of the aircraft is approximately 1000 km and the altitude ceiling is around 4000 m. For this study the mean aircraft speed ranged between 60 and 70 m s^{-1}. A fast response temperature sensor and a nine-hole turbulence probe (BAT probe) were mounted on a boom in front of the aircraft. This instrumental set-up was chosen to reduce flow distortion effects of the aircraft. Measurements of wind and temperature were taken with a frequency of 50 Hz. Other instruments, which were mounted on the aircraft, are a downward-looking video camera to obtain information on the sea surface and ice structure, and an infrared radiometer thermometer (IRT) for measurement of the surface temperature. The atmospheric humidity was measured with a cooled-mirror dew point hygrometer. For the determination of radiative fluxes, upward- and downward looking pyranometers (for short wave radiation) and pyrgeometers (for long wave radiation) were installed. Aircraft position, altitude, attitude and velocity information were obtained from GPS and radar altimeter measurements. A detailed description of the instrumentation and the raw data processing is given by *King et al.* [2008].

2.2. Study Area

[5] Measurements were carried out in 2007 and 2008 during the Antarctic summer months of February and March. The aircraft was operated from Rothera Research Station on Adelaide Island (67.6°S, 68.1°W), which is shown in Figure 1. The black lines in Figure 1 show the flight tracks from the research station to the sea ice areas

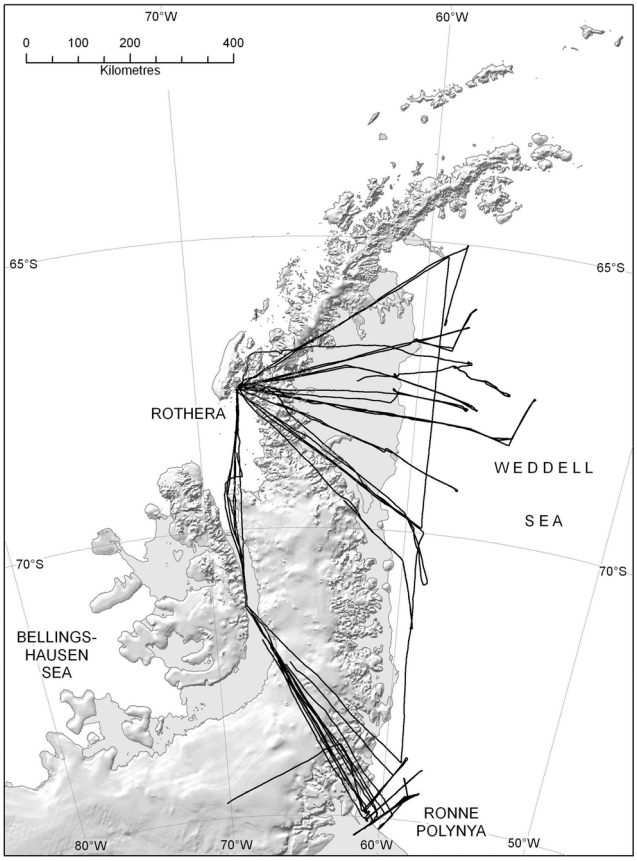

Figure 1. Antarctic Peninsula with flight tracks (black lines) from Rothera research station to the western Weddell Sea ice zone.

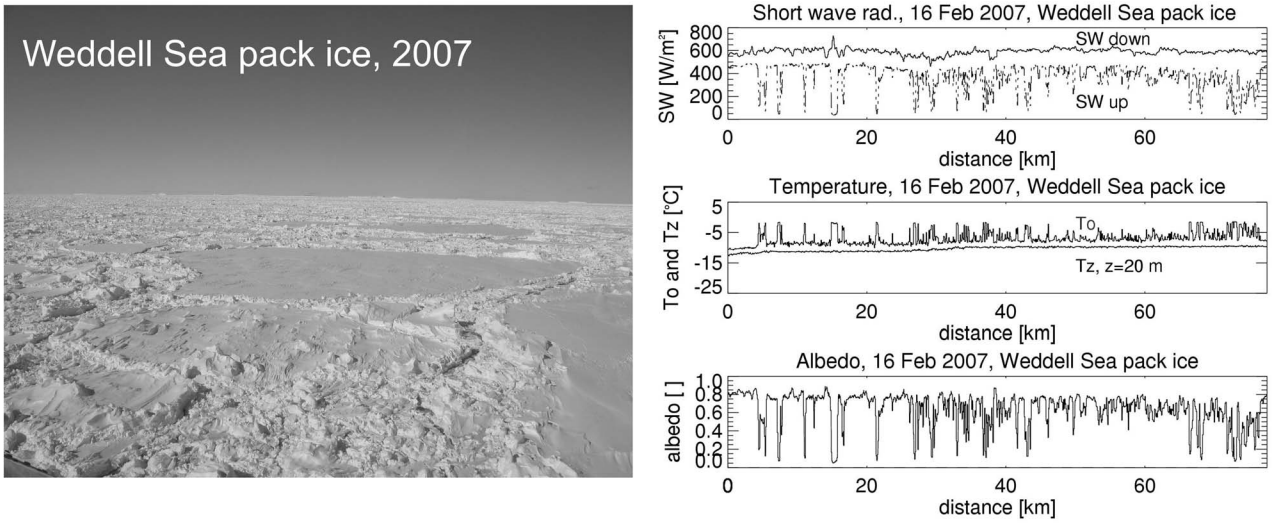

Figure 2. (left) Example of sea ice structure in the western Weddell Sea, photograph taken from the aircraft cockpit at a height of 20 m. (right) (top) Spatial variation of upward and downward directed short wave radiation S_w, (middle) flight level temperature T_z (z = 20 m) and surface temperature T_0, and (bottom) albedo, measured over western Weddell Sea pack ice on 16 February 2007.

in the Weddell Sea. Over sea ice, low level horizontal flight tracks were flown to measure boundary layer parameters. In total, 16 flight missions, conducted over Weddell Sea ice, in the area 65°S–70°S, 55°W–65°W, form the basis of this study.

2.3. Sea Ice Characteristics

[6] Sea ice in the western Weddell Sea can be divided broadly into two different classes: (1) relatively thick and rough "multiyear pack ice," mostly found eastward of and adjacent to the Larsen Ice Shelf and (2) thinner, smoother "young/new sea ice," generally found adjacent to the Ronne Ice Shelf.

[7] Multiyear pack ice is generally less common in the Antarctic than in the Arctic but is found in the western Weddell Sea, which contains approximately 80% of the multiyear sea ice in the Antarctic. A reason for the existence of multiyear ice in the western Weddell Sea is the Weddell Gyre, a clockwise circulating current, which traps sea ice along the eastern side of the Antarctic Peninsula, allowing it to survive for more than one year. For this study we collected boundary layer parameters over the pack ice area during 12 flight missions. The sea ice concentration during these 12 flight missions ranged from 95% to 100%. A picture of typical ice conditions in the western Weddell Sea pack ice area during our observations is shown in Figure 2 (left). The pack ice area shows ridges and in summer areas of open water (leads) between the ice floes which, at times, become covered with thin smooth, newly formed ice. Figure 2 (right) shows an example of the spatial variation of upward and downward directed short wave radiation S_w, surface temperature T_0, flight level temperatures T_z and surface albedo α, measured over pack ice in the western Weddell Sea. The surface temperature and outgoing short wave radiation reflect the heterogeneity of the ice-covered surface in the pack ice region. This heterogeneity of the sea surface results in a strongly variable albedo, which varied during this example from around 0.1 over newly formed dark ice to more than 0.8 over thick snow covered multiyear pack ice.

[8] In the southern part of the western Weddell Sea, we observed smooth new, young or first-year sea ice in the area of the Ronne Polynya, adjacent to the Ronne Ice Shelf. Polynyas (large, persistent areas of open water within the pack ice) cover up to 20% of the overall Antarctic sea ice region. In the Ronne Polynya region, persistent offshore winds and the prevailing ocean current act to drive the newly forming thin ice away from the Ronne Ice Shelf. This area is therefore an important ice production area of the Weddell Sea. In total we flew four flight missions northward from the Ronne Ice Shelf over the polynya and adjacent sea ice. The sea ice concentration during these four flight missions ranged from 98%–100%. During two of these flights cold air flowed off the Ronne Ice Shelf toward the sea and we observed the polynya area nearly completely covered with newly formed ice as shown in Figure 3 (left). Figure 3 (right) shows the corresponding temperatures and short wave radiation fluxes that we observed during that flight mission. The labels on the x-axes denote the flight distance from the Ronne Ice Shelf. The newly formed thin ice had an albedo of less than 0.2. Such thin sea ice is also referred to as nilas. The albedo of snow-free nilas is close to that of open water but increases with increasing ice thickness. Figure 3 (right) shows clearly that in the first 30 km distance from the Ronne Ice Shelf the albedo in the polynya region increased whereas the surface temperature decreased. A reason for this is that with larger distance from the shelf more water freezes on the bottom of the ice, i.e., is increasing the thickness of congelation ice.

3. Aircraft Data

3.1. Roughness Lengths From Aircraft Data

[9] The aerodynamic roughness length z_0 and the scalar roughness length for temperature z_T can be determined by

$$z_0 = z\left[\exp\left(\left(\frac{\rho k^2 u^2}{\tau}\right)^{\frac{1}{2}} + \psi_M\left(\frac{z}{L}\right)\right)\right]^{-1} \quad (1)$$

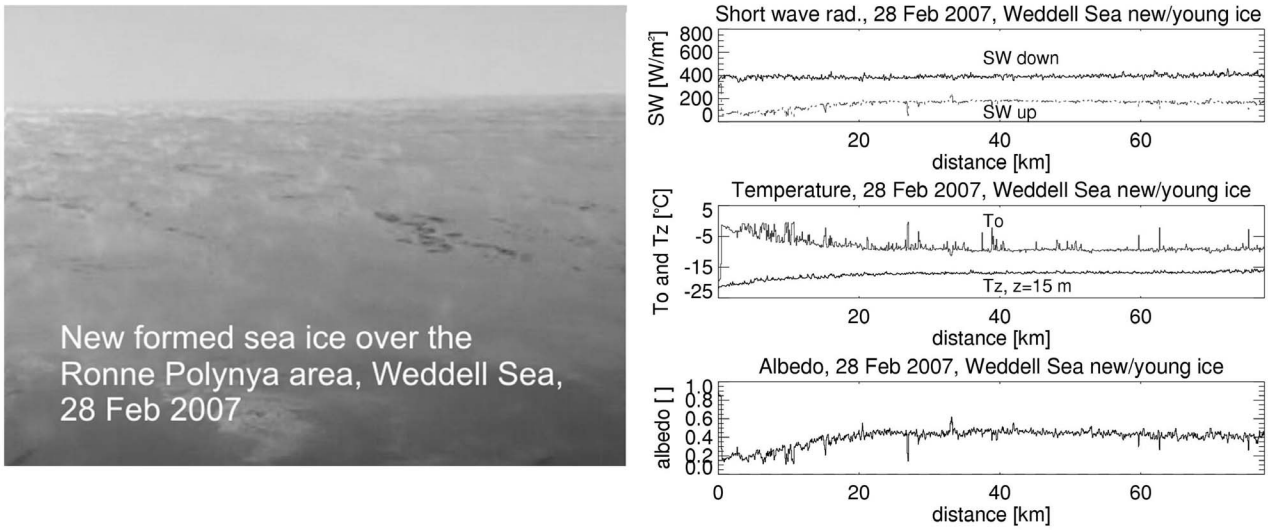

Figure 3. (left) Photograph of newly formed sea ice in the area of the Ronne Polynya, Weddell Sea, taken from the aircraft cockpit at 15 m altitude. (right) (top) Spatial variation of upward and downward short wave radiation (middle) S_w, air temperature T_z (z = 15 m) and surface temperature T_0, and (bottom) albedo measured in the area of the Ronne Polynya, 28 February 2007.

$$z_T = z\left[\exp\left(\frac{\rho c_p k^2 (T_o - T_z)u}{H\left[\ln\left(\frac{z}{z_o}\right) - \psi_M\left(\frac{z}{L}\right)\right]} + \psi_H\left(\frac{z}{L}\right)\right)\right]^{-1} \quad (2)$$

where z is the height at which the wind speed, u, and air temperature, T_z, are measured; ρ is the air density, c_p the specific heat of air at constant pressure, T_0 surface temperature, C_{Dz} the transfer coefficient for momentum and C_{Hz} for sensible heat, L the Obukhov length, and k is the Von Kármán constant. We assume for the Von Kármán constant k a value of 0.4 for momentum as well as for temperature. τ denotes the turbulent momentum flux, H the sensible heat flux. ψ_M and ψ_H are profile functions which accounts for stratification effects.

[10] The profile functions ψ_M and ψ_H in equations (1) and (2) are the integral of gradient functions for momentum ϕ_M and sensible heat ϕ_H, respectively. The Monin Obukhov Theory states, that the profiles of temperature and wind in the atmospheric surface layer can be expressed as function of the stability parameter z/L alone. The gradient functions, also called similarity functions or universal functions, are related to the profile functions ψ_M and ψ_H by *Paulson* [1970]:

$$\psi_F\left(\frac{z}{L}\right) = \int_0^{z/L} \frac{1 - \phi_F(z/L)}{(z/L)} d(z/L) \quad (3)$$

The index F denotes the turbulent fluxes of heat and momentum, respectively.

[11] A wide range of universal ϕ_F functions has been determined empirically from various field experiments and laboratory studies and there still exists controversy regarding the exact form of the profile functions. Several authors [e.g., *Högström*, 1988] discuss typical forms of ϕ_F functions. We use for ψ_M and ψ_H for the unstable stratification functions given by *Paulson* [1970], which are based on the work of *Businger* [1966] and A. J. Dyer (unpublished formula), while for stable stratification, we use the functions of *Holtslag and DeBruin* [1988].

[12] The input parameters on the right-hand side of equations (1) and (2) can be obtained from the aircraft measurements which are described in section 2.1: The surface temperature T_0 is obtained from the IRT measurements. The high-frequency BAT probe measurements of temperature and wind components enables us to compute mean values of the air temperature T_z and wind u as well as the turbulent fluxes of momentum τ and sensible heat H and hence the Obukhov length L.

3.2. Flight Strategy

[13] The flight strategy influences the accuracy of atmospheric data that are measured with an aircraft. An overview of commonly used flight strategies for boundary layer measurements with their advantages and disadvantages are summarized by *Bange et al.* [2006]. The accuracy of turbulence measurements depends on the averaging length over time or space. For this study we determined area averaged values of various turbulence parameters from low level flight legs. We averaged the 50 Hz aircraft raw data over flight sections of 8 km. We assume that for a distance of 8 km Taylor's hypotheses is fulfilled; that is, we assume that the turbulence is frozen along the flight leg because the aircraft speed of 60 to 70 m s^{-1} is about 1 order of magnitude faster than the mean wind speed in the Weddell Sea boundary layer. *Mann and Lenschow* [1994] discuss the impact of the sampling length on the accuracy of aircraft turbulence data. *Schröder et al.* [2003] investigate the impact of the sampling length in particular for aircraft boundary layer measurements over various sea ice conditions. They show that the uncertainty significantly increases for sampling lengths less than 8 km. Not only the sampling length but also the height of the airborne measurement is relevant for the accuracy of boundary layer data. In order to get accurate area representative data over heterogeneous surfaces, such as the ice-covered sea surface,

Table 2. Example of Sensitivity of the Effective Roughness Lengths to Measurement Uncertainties in Sensible Heat Flux H, Momentum Flux τ, Temperature Difference ΔT, and Wind Speed u[a]

Input Parameter	$z_{0_}$eff (m)	$z_{T_}$eff (m)
H, τ, ΔT, u	5.56×10^{-05}	1.67×10^{-05}
H + 20%	5.56×10^{-05}	1.45×10^{-05}
H − 20%	5.56×10^{-05}	8.01×10^{-05}
τ + 25%	1.92×10^{-04}	4.06×10^{-06}
τ − 25%	9.21×10^{-06}	8.31×10^{-05}
ΔT + 0.5	5.56×10^{-05}	1.57×10^{-06}
ΔT − 0.5	5.56×10^{-05}	1.78×10^{-04}
u + 0.1	4.35×10^{-05}	1.67×10^{-05}
u − 0.1	7.11×10^{-05}	1.67×10^{-05}

[a]The chosen reference values are from an 8-km sample, measured over Weddell Sea pack ice at a height of 42 m on 9 February 2008 at 18:14 UTC. The reference values of this example are H = 17.69 W m^{-2}, $\tau = 3.39 \times 10^{-02}$ N m^{-2}, u = 4.9 m s^{-1}, ΔT = 2.6 K.

effective parameters have to be measured above the blending height [*Beljaars and Holtslag*, 1991]. *Vihma* [1995] showed that over a heterogeneous sea ice cover the atmospheric stratification can have a strong effect on the blending height but in heterogeneous terrain the blending height depends mainly on the distance between obstacles or surface changes. The blending height is approximately 1/100 to 1/200 of the characteristic horizontal length scale, according to *Mason* [1988]. We assess that the typical horizontal length scale, characterized by surface changes, of Weddell Sea ice range between 20 m to up to 5 km. In order to collect the airborne data above the blending height we choose flight levels in the range of 15 m to 60 m.

3.3. Data Pre-processing

[14] We pre-processed the aircraft turbulence data in order to improve their accuracy: To minimize systematic errors in the wind measurements, we considered the results of in-flight calibration of the BAT turbulence probe, as described, e.g., by *Lenschow* [1986] and *Williams and Marcotte* [2000]. Furthermore, we applied the aircraft up-wash correction of *Crawford et al.* [1996]. To increase the accuracy of the IRT raw data, we accounted for errors due to emission and absorption effects of atmospheric gases: First, we only used data which we collected during low level flight legs, so that the absolute error due to absorption and emission is relatively small. Second, we applied a similar correction method to that described by *Burns et al.* [2000]; that is, we corrected the infrared temperature data by a factor of ±0.001 K/m. This factor was empirically determined from measurements during descents and ascents over Weddell Sea ice.

[15] Before computing the roughness lengths with equations (1) and (2) we filtered the turbulence data to get reliable signal-to-noise ratios. We limited our analysis to cases for which the mean friction velocity $u_* \geq 0.05$ m s^{-1}, mean wind speed $u \geq 1$ m s^{-1}, mean temperature differences between surface and flight leg $|\Delta T| \geq 0.5$ K and sensible heat flux $|H| \geq 5$ W m^{-2}. Any values of $z_{0_}$eff > 0.1 m were rejected, because they are physically not plausible. We include the rejection for the small temperature differences $|\Delta T| \geq 0.5$ K also in the determination of the aerodynamic roughness length in order to obtain data for both roughness lengths for each 8-km samples of the low level flight legs. These data selection criteria are similar to those used by *Andreas et al.* [2005] when analyzing surface-based measurements from the Weddell Sea pack ice region. The selection criteria reduce our data measured over rough pack ice to 115 eight-kilometer samples, and over smooth new/young first-year ice to 48 eight-kilometer samples.

3.4. Measurement Uncertainty

[16] An overview of possible errors in aircraft flux measurements is discussed by *Mahrt* [1998]. Even after pre-processing of the data as described in section 3.3, measurement errors in mean wind, temperature and turbulent fluxes can still contribute to an uncertainty in estimates of $z_{0_}$eff and $z_{T_}$eff. *Garman et al.* [2006] investigated the uncertainty of the wind measurements by testing a BAT probe in a wind tunnel. They assessed that the precision of the vertical wind measurements w due to instrument noise was approximately ±0.03 m/s. *Garman et al.* [2008] showed that an additional uncertainty in the wind data results when a constant up-wash correction value is used, as proposed by the model of *Crawford et al.* [1996]. The use of a constant up-wash correction increases the uncertainty in w to approximately ±0.05 m/s. We assume for the other two wind components, u and v, similar high uncertainties due to aircraft movement. With further random error sources, such as icing and water problems and uncertainties in the GPS measurements, we assess the total measurement error of the turbulent momentum fluxes to be up to 25% and of the sensible heat flux to be 20%. The accuracy of the air temperature measurements can be impaired due to random errors in recovery correction, calibration, instrument drift and sensor wetting. The accuracy of the surface temperature measured with the IRT is limited, because a mean sea surface emissivity has to be assumed. Therefore, we assess that the accuracy of ΔT is about ±0.5 K. To summarize this estimate of uncertainty and to give an idea of numbers, we calculate in Table 2 an explicit example for the sensitivity of the effective aerodynamic roughness length and the scalar roughness length for temperature to aircraft measurement errors. Table 2 shows that the main uncertainty for the determination of the aerodynamic roughness length arises from the measurement uncertainty of the momentum flux, whereas for the scalar roughness length for temperature the measurement uncertainty of sensible heat flux and of the temperature difference ΔT make the largest contributions.

[17] It has to be mentioned that there exists not only an uncertainty due to measurement errors in H and M but also due to the assumptions which are made for calculating the turbulent fluxes with the Monin Obukhov Theory. One example of such an uncertainty results from the fact that there exists a variety of published profile functions for H and M. This uncertainty is related to the atmospheric stability and is discussed in detail, e.g., by *Weidinger et al.* [2000] and *Weiss* [2002].

4. Effective Roughness Lengths of Weddell Sea Ice

[18] Figure 4 shows scatterplots of $z_{0_}$eff versus $z_{T_}$eff for Weddell Sea pack ice (Figure 4, left) and new/young Weddell Sea ice (Figure 4, right), calculated for 8-km flight segments (triangles). It is seen in Figure 4 that both roughness lengths over both sea ice areas are highly variable: They show a large scatter, range over several orders of magnitude and are not

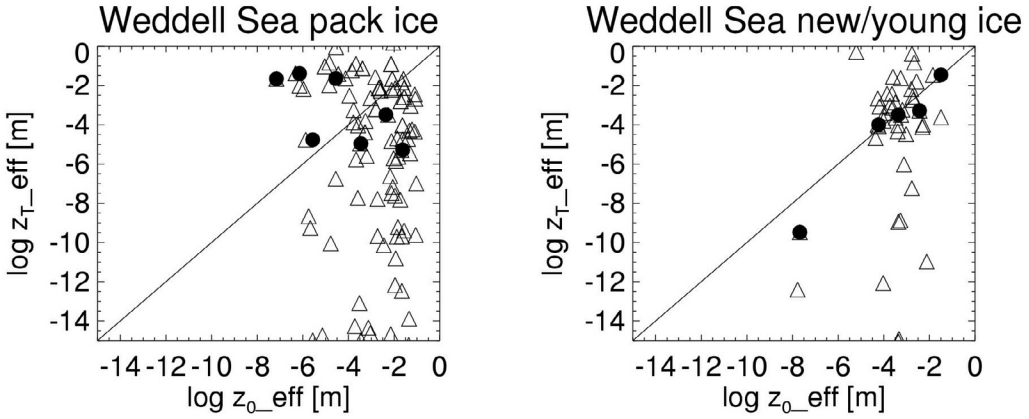

Figure 4. Triangles show scatterplot of 8-km-averaged values of effective aerodynamic roughness length versus scalar roughness length of temperature of (left) Weddell Sea pack ice and (right) new/young Weddell Sea ice. A bin is defined as $\Delta\log z\_\text{eff} = 0.1$ m wide. The solid line represents a perfect correlation; the black dots show the scatterplot of bin-averaged values.

equal. The scatter can partly be a result of remaining measurement uncertainties. Beside the measurement uncertainties which are described in section 3.4, the measurements can also been impaired by low level jets. Low level jets can develop in the boundary layer over Weddell Sea ice [e.g., *Andreas et al.*, 2000]. If the aircraft is collecting data below, in or above a low level jet the wind speed can significantly change and hence, the measurements could give too small or too large values of z_0_eff, when determined by equation (1) and of z_T_eff when determined by equation (2). Although the scatter can partly be a result of remaining measurement uncertainties, one main reason for this scatter might also be the heterogeneity of the sea ice surface in the meso-scales. Geometric roughness and temperature differences can be observed between different locations on the sea surface even when the sea ice type remains the same. For example, we observed in the southern pack ice area larger geometrical pressure ridges than further north. The 8-km samples in Figure 4 show that z_0_eff can be larger than z_T_eff as well as smaller than z_T_eff for both sea ice categories. Both behaviors of z_0_eff relative to z_T_eff were observed in previous studies: On the one hand, previous studies over heterogeneous surfaces and sea ice showed that the aerodynamic roughness length can be larger than the scalar roughness lengths for temperature [*Garratt*, 1978; *Schröder et al.*, 2003]. On the other hand, in contradiction to this, observations over snow covered surfaces [*Calanca*, 2001; *King and Anderson*, 1994] showed that the scalar roughness length for temperature can be 10 to 100 times larger then the aerodynamic value.

[19] To determine typical ratios of both roughness lengths for Weddell Sea ice, we bin-averaged the data in Figure 4 in order to increase the statistical significance of the results. We define that a bin is $\Delta\log z\_\text{eff} = 0.1$ m wide. Figure 4 (right) shows the bin-averaged values (solid dots) measured in the new/young ice area. The bin-averaged roughness length values for the new/young sea ice show less scatter. Figure 4 (left) shows that the bin-averaged roughness length values of the pack ice area still show a large scatter, i.e., z_T_eff can be significant smaller as well as larger relative to z_0_eff within a bin. Greater local differences in the sea ice structure of the pack ice, e.g., in the surface geometry, may be the reason for this scatter. Moreover, recent publications show that the roughness lengths are not only a function of surface geometric parameters, as assumed in classic boundary layer theories, but can be also a function of friction velocity and snow drift [*Smeets and van den Broeke*, 2008a, 2008b], atmospheric stability [*Zilitinkevich et al.*, 2008] or temperature defect [*Calanca*, 2001]. Local differences in these factors may therefore be responsible for some of the scatter in Figure 4. However, most numerical models cannot take small or local scale variations of the roughness lengths over a certain surface type into account. Instead a typical value of the aerodynamic and the scalar roughness length for a certain surface or sea ice type is assumed as input parameters for the bulk parameterizations.

[20] We calculated from the data shown in Figure 4 the average median roughness lengths for each sea ice area and listed them in Table 3. The averaged effective value of the temperature roughness length of the new/young sea ice area is $\overline{z_T\_\text{eff}} = 2.2 \times 10^{-04}$ m. This value is one order of magnitude larger than the averaged value of $\overline{z_T\_\text{eff}} = 1.8 \times 10^{-05}$ m of the pack ice area. The effective aerodynamic roughness length for Weddell Sea the new/young sea ice area is $\overline{z_0\_\text{eff}} = 4.5 \times 10^{-04}$ m, and is about one order of magnitude smaller than the median value of $\overline{z_0\_\text{eff}} = 4.1 \times 10^{-03}$ m of pack ice. It is not surprising, that the averaged values of the aerodynamic roughness lengths of the new/young sea ice area are smaller than that of the pack ice area, because the geometric roughness of young ice surfaces is in general much smoother than the multiyear pack ice cover.

[21] The data listed in Table 3 show that for new/young sea ice $\overline{z_T\_\text{eff}}$ is the same order of magnitude but about half the value of $\overline{z_0\_\text{eff}}$. Averaged over all pack ice data $\overline{z_T\_\text{eff}}$ is in the range of 2 orders of magnitude smaller than $\overline{z_0\_\text{eff}}$. In general, our data show that the averaged value of z_T_eff is smaller than the averaged value of $\overline{z_0\_\text{eff}}$ for Weddell Sea ice. The reason for the difference between the aerodynamic and the scalar roughness length of temperature is that different physical processes are responsible for temperature and wind profile development, as described for example by *Brutsaert* [1975]. The main difference results from the fact that near the surface momentum is transferred by diffusion

Table 3. Experimentally Determined Roughness Lengths of Snow Covered Surfaces in the Antarctic

Experiment	Surface Type, Location (n of 8-km Samples)	Season	Average Value z_0 (m)	Average Value z_T (m)
This study	New/young ice area Weddell Sea (48)	Summer 2007 and 2008	4.5×10^{-4} (median) $\sigma_{z0} = 0.051$	2.2×10^{-4} (median) $\sigma_{zT} = 0.098$
This study	Pack ice Weddell Sea (115)	Summer 2007 and 2008	4.1×10^{-2} (median) $\sigma_{z0} = 0.02$	1.8×10^{-5} (median) $\sigma_{zT} = 0.166$
Bintanja and Reijmer [2001]	Inland snow- covered surface	Summer 1997/1998	$(2.0 \pm 1) \times 10^{-4}$	$(2.0 \pm 1) \times 10^{-4}$
Wamser and Martinson [1993]	Pack ice Weddell Sea	Winter 1986	4.7×10^{-2} (median)	No data
		Winter 1989	2.7×10^{-2} (median)	No data

and pressure, and these are therefore also the physical processes which influence $\overline{z_0\_\text{eff}}$, whereas temperature is solely transferred from the surface by diffusion and hence is the dominant physical process influencing $\overline{z_T\_\text{eff}}$. *Beljaars and Holtslag* [1991] showed over land that the effective roughness length for temperature is drastically reduced when inhomogeneous terrain effects increase the aerodynamic roughness lengths. Their study indicates that small areas of large roughness length dominate the momentum transfer whereas the heat transfer is still determined by the characteristics of the dominant surface cover. This might also be valid in particular for the relatively rough pack ice area and it explains why we observed that $\overline{z_T\_\text{eff}}$ is in this sea ice area two orders of magnitude smaller than $\overline{z_0\_\text{eff}}$.

5. Summary and Discussion

[22] This study is based on aircraft measurements in two different Antarctic sea ice areas (pack ice and new/young sea ice), and it shows that z_T_eff and z_0_eff are highly variable for Weddell Sea ice and can vary over several orders of magnitudes within the same sea ice area. However, most numerical models cannot take small scale variations of the roughness length into account. They still use a constant value of the aerodynamic and scalar roughness lengths for a certain surface type as boundary input parameters for the calculation of the turbulent energy fluxes. Due to the fact that up to now there are only scanty experimental data of areally averaged roughness lengths in the Antarctic Sea ice zone, this study aims to determined averaged values of z_T_eff and z_0_eff for Weddell Sea ice from aircraft measurements. Effective roughness lengths over heterogeneous and complex terrain like sea ice can differ from local point measurements because in such terrain, point measurements do not represent the whole area but only an upstream fetch, as described, e.g., by *Mahrt and Ek* [1993] or *Schmid* [1994]. Therefore, effective values of the roughness length are appropriate to be used as input parameters for numerical model studies, because they can be representative for an area the size of a model grid box.

[23] In Table 3 we give median values of the effective roughness lengths of pack ice and new/young Weddell Sea ice, respectively. For a comparison we also list in Table 3 roughness length values from previous Antarctic studies. Regarding the scalar roughness length, we observed a similar mean $\overline{z_T\_\text{eff}}$ value in the new/young sea ice area to that which *Bintanja and Reijmer* [2001] observed at an inland snow covered Antarctic surface in the absence of snow drift, i.e., a value in the order of 2×10^{-04} m. This indicates that the heat transfer in particular is determined by the characteristics of the dominant surface cover as already pointed out in the study by *Beljaars and Holtslag* [1991]. The $\overline{z_T\_\text{eff}}$ value of new/young sea ice is about one order of magnitude larger than the value for pack ice. The averaged effective aerodynamic roughness lengths that we observed in the pack ice area are of the same order of magnitude as the z_0 values that *Wamser and Martinson* [1993] observed using ground-based measurements in the Weddell Sea pack ice area in winter. The slight difference of our aerodynamic roughness length values to the mean values given by *Wamser and Martinson* [1993] for their winter experiment 1989 might not only be due to the different experiment season but also due to the fact that they measured local values at the ground and our study determined effective roughness lengths. Due to the nonhomogeneity of the ice-covered Weddell Sea surface, it can be assumed that internal boundary layers develop. The internal boundary layer is in particular influenced by the physical height of different roughness elements and by the friction velocity at both sides of roughness jumps. *Rao et al.* [1974] describe the influence of a sudden change in surface roughness on the boundary layer structure. Moreover, the differences in the surface temperature values, which are quite significant over Weddell Sea pack ice, as illustrated in Figure 2, lead additionally to a development of thermal internal boundary layers. In the presence of internal boundary layers ground based mast or buoy measurements often catch local rather than area-representative atmospheric values. A second reason for the slight differences of our summer data to the winter 1989 aerodynamic roughness length data of *Wamser and Martinson* [1993] might be caused by different snow cover on the sea ice. Melting snow in summer can increase the roughness of snow covered surfaces, as discussed by *Smeets and van den Broeke* [2008a] for the ablation zone of a Greenland ice sheet, where the snowmelt uncovered hummocky ice or as discussed by *Andreas et al.* [2010] for Arctic summer sea ice, where leads and melt ponds create vertical ice faces which enhance the form drag.

[24] For both sea ice areas in the Weddell Sea our study show that the averaged value of $\overline{z_T\_\text{eff}}$ is smaller than the averaged value of $\overline{z_0\_\text{eff}}$. Most models still work with the assumption that both roughness lengths are equal. The ratio between the two roughness lengths is relatively small for new/young sea ice where we observed $\overline{z_0\_\text{eff}}/\overline{z_T\_\text{eff}} \approx 2$, but the ratio becomes significantly larger for pack ice, where we measured $\overline{z_0\_\text{eff}}/\overline{z_T\_\text{eff}} \approx 227$. *Schröder et al.* [2003] observed effective roughness lengths of sea ice in the Baltic Sea and in the Fram Strait. They also observed that the effective scalar roughness length is, in general, smaller than

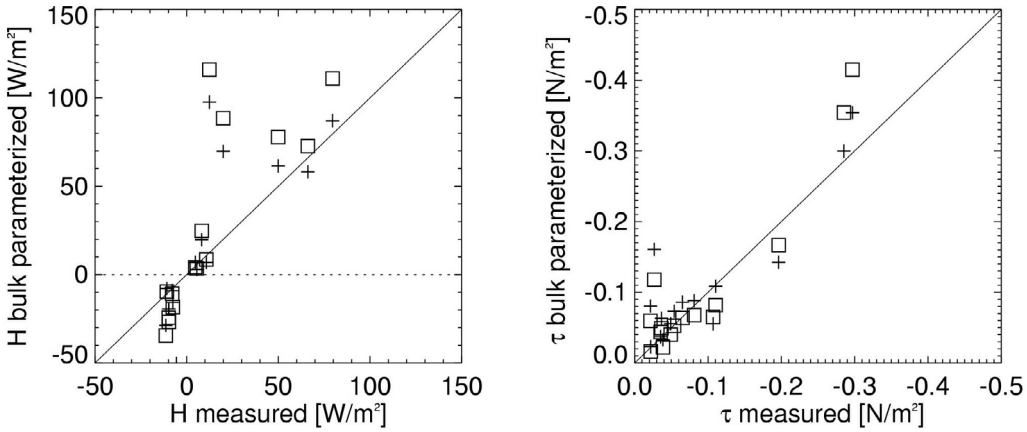

Figure 5. Squares show scatterplot of (left) measured turbulent sensible heat flux H versus bulk parameterized H and (right) measured momentum flux τ versus bulk parameterized τ using roughness length values of $z_0 = z_T = 0.001$ (squares). Crosses show the same scatterplot but with bulk parameterized fluxes using mean roughness length values for Weddell Sea ice from this study, i.e., for the new/young area $z_0\_\mathrm{eff} = 4.5 \times 10^{-4}$ m and $z_T\_\mathrm{eff} = 2.2 \times 10^{-4}$ m, for the pack ice area $z_0\_\mathrm{eff} = 4.1 \times 10^{-3}$ m and $z_T\_\mathrm{eff} = 1.8 \times 10^{-5}$ m. Each symbol represents the averaged turbulent fluxes of one flight mission.

the effective aerodynamic roughness length. However, the magnitude of the ratio of $\overline{z_0\_\mathrm{eff}/z_T\_\mathrm{eff}}$ for northern hemispheric sea ice differs significantly in comparison to our results for Antarctic sea ice: The measurements of *Schröder et al.* [2003] show that for gray, young ice the ratio is $\overline{z_0\_\mathrm{eff}/z_T\_\mathrm{eff}} \approx 2000$ and for very rough multiyear ice the ratio becomes $\overline{z_0\_\mathrm{eff}/z_T\_\mathrm{eff}} \approx 250{,}000$. Theses ratios are much larger than those we found for similar ice classes in the Antarctic Weddell Sea. The differences in the ratios of the roughness lengths between northern hemispheric/Arctic sea ice and Antarctic sea ice show that sea ice parameters determined in the Arctic are often not transferable to describe Antarctic sea ice areas.

[25] The ratios of the roughness lengths of the Weddell Sea ice areas show, that the assumption that both roughness lengths are equal, like it is still common in numerical models, is not appropriate for simulations for sea ice areas, in particular not for the pack ice region. Examples of models which work with this assumption that both roughness lengths are equal are the ECHAM3 atmospheric general circulation model [*Deutsches Klimarechenzentrum*, 1992], the HadGEM1 model [*Johns et al.*, 2005] or the Polar MM5, as described by *Guo et al.* [2003]. The ECHAM3 assumes that both roughness lengths are uniform with a value of 1.0×10^{-03} m over sea ice. In the MM5 surface layer scheme no thermal roughness length parameterization is included [*Skamarock et al.*, 2008] and the scalar roughness length is assumed to be equal to the aerodynamic roughness length. The HadGEM1 model [*Johns et al.*, 2005] also works with the assumption that both roughness lengths are equal and they are set to a value of 0.5×10^{-04} m, but this value can be adjusted for different sea ice types from 0.01×10^{-04} m to 0.1 m. Polar MM5 assumes for Antarctic sea ice a single roughness length value also of 1.0×10^{-03} m. The assumption of $z_T = z_0 = 1.0 \times 10^{-03}$ m is quite common in models for sea ice roughness lengths. However, some models uses even higher aerodynamic roughness length, in order to tune and improve the simulated synoptic-scale systems, e.g., for that reason in the HIRLAM model the aerodynamic roughness length of sea ice is set as high as 0.03 m [e.g., *Vihma*, 2009]. By comparing it with our data as listed in Table 3 this assumption is in particular too large to describe the effective scalar roughness length in the Weddell Sea ice areas and the effective aerodynamic roughness length of the new/young sea ice area. Using a too large value for the roughness length can result in an overestimation of the bulk parameterized fluxes over sea ice. Figure 5 compares direct measured turbulent fluxes versus bulk parameterized turbulent fluxes which were calculated, first, with the common model assumption that $z_T = z_0 = 1.0 \times 10^{-03}$ m and, second, with the assumption of the mean roughness length values of this study, as listed in Table 3. Each symbol represents the averaged value for one entire flight mission during our experiments in 2007 and 2008. Figure 5 shows that by using the assumption $z_T = z_0 = 1.0 \times 10^{-03}$ m the parameterized sensible heat flux is in general overestimated and the parameterized momentum flux can be over- or underestimated. By using the mean values for the roughness lengths, as listed in Table 3, the accuracy of the parameterized fluxes can be improved in particular for the southern part of the western Weddell Sea: for this area the root mean square error *RMSE* of the sensible flux decreases from $\mathrm{RMSE}\_H = 36.82$ W m^{-2} to $\mathrm{RMSE}\_H = 23.94$ W m^{-2} and of the momentum flux from $\mathrm{RMSE}\_\tau = 0.065$ N m^{-2} to $\mathrm{RMSE}\_\tau = 0.042$ N m^{-2}. The normalized fractional bias FB becomes smaller for the sensible heat flux from $\mathrm{FB}\_H = 0.5$ to 0.2 and for momentum flux from $\mathrm{FB}\_\tau = 0.13$ to 0.03. For the pack ice region we see only a significant statistical improvement for the sensible heat flux by using the mean value listed in Table 3 and their FB_H decreases from 0.48 to 0.28 and the RMSE_H from 37.1 to 29.95 W m^{-2}. Figure 5 shows that using mean values that are characteristic of a certain sea ice area can significantly improve the accuracy of the parameterized fluxes in the Antarctic Weddell sea ice region.

[26] **Acknowledgments.** The map in Figure 1 was provided by Peter Fretwell. The authors would like to thank the anonymous reviewers and T. Vihma for their helpful comments and discussions.

References

Andreas, E. L., K. J. Claffey, and A. P. Makshtas (2000), Low-level atmospheric jets over the Western Weddell Sea, *Boundary Layer Meteorol.*, *97*, 459–486, doi:10.1023/A:1002793831076.

Andreas, E., R. E. Jordan, and A. P. Makshtas (2005), Parameterizing turbulent exchange over sea ice: The ice station Weddell results, *Boundary Layer Meteorol.*, *114*, 439–460, doi:10.1007/s10546-004-1414-7.

Andreas, E. L., T. W. Horst, A. A. Grachev, P. O. G. Persson, C. W. Fairall, P. S. Guest, and R. E. Jordan (2010), Parameterizing turbulent exchange over summer sea ice and the marginal ice zone, *Q. J. R. Meteorol. Soc.*, *136*, 927–943, doi:10.1002/qj.618.

Bange, J., P. Zittel, T. Spieß, J. Uhlenbrock, and F. Beyrich (2006), A new method for the determination of area-averaged turbulent surface fluxes from low level flights using inverse models, *Boundary Layer Meteorol.*, doi:10.1007/s10546-005-9040-6.

Beljaars, A. C. M., and A. A. M. Holtslag (1991), Flux parameterization over land surfaces for atmospheric models, *J. Appl. Meteorol.*, *30*, 327–341, doi:10.1175/1520-0450(1991)030<0327:FPOLSF>2.0.CO;2.

Bintanja, R., and C. H. Reijmer (2001), A simple parameterization for snowdrift sublimation over Antarctic snow surfaces, *J. Geophys. Res.*, *106*(D23), 31,739–31,748, doi:10.1029/2000JD000107.

Brutsaert, W. (1975), The roughness length for water vapor, sensible heat, and other scalars, *J. Atmos. Sci.*, *32*, 2028–2031, doi:10.1175/1520-0469(1975)032<2029:TRLFWV>2.0.CO;2.

Burns, S. P., et al. (2000), Comparison of aircraft, ship, and buoy radiation and SST measurements from TOGA COARE, *J. Geophys. Res.*, *105*(D12), 15,627–15,652, doi:10.1029/2000JD900090.

Businger, J. A. (1966), Transfer of momentum and heat in the planetary boundary layer, in *Proceedings of the Symposium on. Arctic Heat Budget and Atmospheric Circulation*, pp. 305–331, Rand Corp., Santa Monica, Calif.

Calanca, P. L. (2001), A note on the roughness length for temperature over melting snow and ice, *Q. J. R. Meteorol. Soc.*, *127*, 255–260, doi:10.1002/qj.49712757114.

Claussen, M. (1991), Estimation of areally averaged surface fluxes, *Boundary Layer Meteorol.*, *54*, 387–410, doi:10.1007/BF00118868.

Crawford, T. L., R. J. Dobosy, and E. Dumas (1996), Aircraft wind measurement considering lift-induced upwash, *Boundary Layer Meteorol.*, *80*, 79–94, doi:10.1007/BF00119012.

Deutsches Klimarechenzentrum (DKRZ) (1992), The ECHAM3 atmospheric general circulation model, *DKRZ Tech. Rep. 6*, Modellbetreuungsgruppe, Hamburg, Germany.

Garbrecht, T., C. Lüpkes, J. Hartmann, and M. Wolff (2002), Atmospheric drag coefficients over sea ice-validation of a parameterization concept, *Tellus, Ser. A*, *54*, 205–219, doi:10.1034/j.1600-0870.2002.01253.x.

Garman, K. E., K. A. Hill, P. Wyss, M. Carlsen, J. R. Zimmerman, B. H. Stirm, T. Q. Carney, R. Santini, and P. B. Shepson (2006), An airborne and wind tunnel evaluation of a wind turbulence measurement system for aircraft-based flux measurements, *J. Atmos. Oceanic Technol.*, *23*, 1696–1708, doi:10.1175/JTECH1940.1.

Garman, K. E., P. Wyss, M. Carlsen, J. R. Zimmermann, B. H. Stirm, T. Q. Carney, R. Santini, and P. B. Shepson (2008), The contribution of variability of lift-induced upwash to the uncertainty in vertical winds determined from an aircraft platform, *Boundary Layer Meteorol.*, *126*, 461–476, doi:10.1007/s10546-007-9237-y.

Garratt, J. R. (1978), Transfer characteristic for a heterogeneous surface of large aerodynamic roughness, *Q. J. R. Meteorol. Soc.*, *104*, 491–502, doi:10.1002/qj.49710444019.

Garratt, J. R. (1990), The internal boundary layer–a review, *Boundary Layer Meteorol.*, *50*, 171–203, doi:10.1007/BF00120524.

Guo, Z., D. H. Bromwich, and J. J. Cassan (2003), Evaluation of polar MM5 simulations of Antarctic atmospheric circulation, *Mon. Weather Rev.*, *131*, 384–411, doi:10.1175/1520-0493(2003)131<0384:EOPMSO>2.0.CO;2.

Högström, U. (1988), Non-dimensional wind and temperature profiles in the atmospheric surface layer: A re-evaluation, *Boundary Layer Meteorol.*, *42*, 55–78, doi:10.1007/BF00119875.

Holtslag, A. A. M., and H. A. R. DeBruin (1988), Applied modeling of the nighttime surface energy balance over land, *J. Appl. Meteorol.*, *27*, 689–704, doi:10.1175/1520-0450(1988)027<0689:AMOTNS>2.0.CO;2.

Joffre, S. M. (1983), Determining the form drag contribution to the total stress of the atmospheric flow over ridged sea ice, *J. Geophys. Res.*, *88*(C7), 4524–4530, doi:10.1029/JC088iC07p04524.

Johns, T., et al. (2005) HadGEM1—Model description and analysis of preliminary experiments for the IPCC Fourth Assessment Report, *Tech. Note 55*, Hadley Cent., Exeter, U. K.

King, J. C., and P. S. Anderson (1994), Heat and water vapour fluxes and scalar roughness lengths over an Antarctic ice shelf, *Boundary Layer Meteorol.*, *69*, 101–121, doi:10.1007/BF00713297.

King, J. C., T. A. Lachlan-Cope, R. S. Ladkin, and A. Weiss (2008), Airborne measurements in a stable boundary layer over the Larsen Ice Shelf, Antarctica, *Boundary Layer Meteorol.*, *127*, 413–428, doi:10.1007/s10546-008-9271-4.

Lenschow, D. H. (1986), Aircraft measurements in the boundary layer, in *Probing the Atmospheric Boundary Layer*, edited by D. H. Lenschow, pp. 39–55, Am. Meterorol. Soc., Boston, Mass.

Mahrt, L., and M. Ek (1993), Spatial variability of turbulent fluxes and roughness lengths in HAPEX-MOBILHY, *Boundary Layer Meteorol.*, *65*, 381–400.

Mahrt, L. (1998), Flux Sampling Errors for Aircraft and Towers, *J. Atmos. Oceanic Technol.*, *15*, 416–429, doi:10.1175/1520-0426(1998)015<0416:FSEFAA>2.0.CO;2.

Mann, J., and D. H. Lenschow (1994), Errors in airborne flux measurements, *J. Geophys. Res.*, *99*(D7), 14,519–14,526, doi:10.1029/94JD00737.

Mason, P. J. (1988), The formation of areally averaged roughness length, *Q. J. R. Meteorol. Soc.*, *114*, 399–420, doi:10.1002/qj.49711448007.

Overland, J. E. (1985), Atmospheric boundary layer structure and drag coefficients over sea ice, *J. Geophys. Res.*, *90*(C5), 9029–9049, doi:10.1029/JC090iC05p09029.

Paulson, C. A. (1970), The mathematical representation of wind speed and temperature profiles in the unstable atmospheric surface layer, *J. Appl. Meteorol.*, *9*, 857–861, doi:10.1175/1520-0450(1970)009<0857:TMROWS>2.0.CO;2.

Rao, K. S., J. C. Wyngaard, and O. R. Coté (1974), The structure of the two-dimensional internal boundary layer over a sudden change of surface roughness, *J. Atmos. Sci.*, *31*, 738–746, doi:10.1175/1520-0469(1974)031<0738:TSOTTD>2.0.CO;2.

Schmid, H. P. (1994), Source areas for scalars and scalar fluxes, *Boundary Layer Meteorol.*, *67*, 293–318, doi:10.1007/BF00713146.

Schröder, D., T. Vihma, A. Kerber, and B. Brümmer (2003), On the parameterization of turbulent surface fluxes over heterogeneous sea ice surfaces, *J. Geophys. Res.*, *108*(C6), 3195, doi:10.1029/2002JC001385.

Skamarock, W. C., J. B. Klemp, J. Dudhia, D. O. Gill, D. M. Barker, M. G. Duda, X.-Y. Huang, W. Wang, and J. G. Powers (2008), A description of the advanced research WRF Version 3, *NCAR Tech. Note NCAR/TN-475+STR*, Natl. Cent. for Atmos. Res., Boulder, Colo.

Smeets, C. J. P. P., and M. R. van den Broeke (2008a), Temporal and spatial variation of momentum roughness length in the ablation zone of the Greenland ice sheet, *Boundary Layer Meteorol.*, *128*(3), 315–338, doi:10.1007/s10546-008-9291-0.

Smeets, C. J. P. P., and M. R. van den Broeke (2008b), The parameterization of scalar transfer over rough ice, *Boundary Layer Meteorol.*, *128*(3), 339–355, doi:10.1007/s10546-008-9292-z.

Taylor, P. A. (1987), Comments and further analysis on the effective roughness length for use in numerical three-dimensional models: A research note, *Boundary Layer Meteorol.*, *39*, 403–418, doi:10.1007/BF00125144.

Vihma, T. (1995), Subgrid parameterization of surface heat and momentum fluxes over polar oceans, *J. Geophys. Res.*, *100*, 22,625–22,646, doi:10.1029/95JC02498.

Vihma, T. (2009), Modelling of the atmospheric boundary layer over sea ice, *HIRLAM Newsl.*, *48*, Article 19.

Wamser, C., and D. G. Martinson (1993), Drag coefficients for winter Antarctic pack ice, *J. Geophys. Res.*, *98*(C7), 12,431–12,437, doi:10.1029/93JC00655.

Weidinger, T., J. Pinto, and L. Horváth (2000), Effects of uncertainties in universal functions, roughness length, and displacement height on the calculation of surface layer fluxes, *Meteorol. Z.*, *9*(3), 139–154.

Weiss, A. (2002), Determination of thermal stratification and turbulence of the atmospheric surface layer over various types of terrain by optical scintillometry, Ph.D. thesis, *Swiss Fed. Inst. of Technol.*, Zurich.

Williams, A., and D. Marcotte (2000), Wind measurements on a maneuvering twin engine turboprop aircraft accounting for flow distortion, *J. Atmos. Oceanic Technol.*, *17*, 795–810, doi:10.1175/1520-0426(2000)017<0795:WMOAMT>2.0.CO;2.

Zilitinkevich, S. S., I. Mammarella, A. A. Baklanov, and S. M. Joffre (2008), The effect of stratification on the aerodynamic roughness length and displacement height, *Boundary Layer Meteorol.*, *129*, 179–190, doi:10.1007/s10546-008-9307-9.

J. King, T. Lachlan-Cope, R. Ladkin, and A. I. Weiss, British Antarctic Survey, National Environment Research Council, High Cross, Madingley Road, Cambridge CB3 0ET, UK. (jcki@bas.ac.uk; tlc@bas.ac.uk; rsla@bas.ac.uk; aiw@bas.ac.uk)